

Supporting Information for

# Comparison of the Different Responses of Surface Plasmon Resonance and Quartz Crystal Microbalance under Various Experimental Scenarios at Solid-Liquid Interfaces

*Jiajie Fang, † Chunlai Ren, † Tao Zhu, † Kaiyu Wang, † Zhongying Jiang<sup>‡†\*</sup>, Yuqiang Ma<sup>†§\*</sup>*

<sup>†</sup>National Laboratory of Solid State Microstructures and Department of Physics, Nanjing University,  
Nanjing 210093, China

<sup>‡</sup>School of Electronics and Information and College of Chemistry and Biological Science, Yi Li  
Normal University, Yining 83500, China

<sup>§</sup>Laboratory of Soft Condensed Matter Physics and Interdisciplinary Research, Soochow University,  
Suzhou 215006, China

\*Authors to whom correspondence should be addressed. Tel and e-mail: (086)13813955964;

jiangzhying@163.com(Z. Y. Jiang) and (086)02583592900, myqiang@nju.edu.cn(Y. Q. Ma).

## SI 1: An Overview of SPR and QCM

The constitution of SPR is shown in Figure 1 (A). The single adsorbed layer is sandwiched between a metallic film and semi-infinite bulk solution. The reflectance  $R$  of a p-polarized light incident upon the metal film through a glass prism (or hemisphere), has the form<sup>1,2</sup>

$$R = |r|^2 = \left| \frac{(M_{11} + M_{12}q_b)q_p - (M_{21} + M_{22}q_b)}{(M_{11} + M_{12}q_b)q_p + (M_{21} + M_{22}q_b)} \right|^2 \quad (S1)$$

$$\begin{bmatrix} M_{11} & M_{12} \\ M_{21} & M_{22} \end{bmatrix} = \begin{bmatrix} \cos(\beta_m) & -i \sin(\beta_m)/q_m \\ -iq_m \sin(\beta_m) & \cos(\beta_m) \end{bmatrix} \begin{bmatrix} \cos(\beta_f) & -i \sin(\beta_f)/q_f \\ -iq_f \sin(\beta_f) & \cos(\beta_f) \end{bmatrix} \quad (S2)$$

$$q_k = \frac{\sqrt{\varepsilon_k - \varepsilon_p \sin^2 \theta}}{\varepsilon_k} \quad \beta_k = h_k \frac{2\pi}{\lambda} \sqrt{\varepsilon_k - \varepsilon_p \sin^2 \theta}$$

where  $h$ ,  $\varepsilon$  and  $\lambda$  are the thickness, dielectric constant, and wavelength, subscript p, m, f and b are the abbreviation of glass prism, metallic film, adsorbed film and bulk solution, respectively, k refers to f or b.

With increasing incident angle, the value of  $R$  calculated from equation 1 holds at about 1, drops sharply to a minimum, and increases back quickly. The physics of this decrease is, the evanescent field couples with the surface free electrons (surface plasma excitations) and drives them to resonate.<sup>3,4</sup> The intensity of the reflected light is then significantly reduced. This evanescent field is generated in case the incident angles are larger than the critical angle.

The specific value of angle  $\theta$  at which  $R$  approaches the minimum is very sensitive to the optical properties of the layer on top of the thin metallic film. In the thin limit, it has

$$\Delta\theta \approx \frac{4\pi}{\lambda n_b^2 \cos \theta} \left( \frac{\varepsilon_m \varepsilon_b}{\varepsilon_m + \varepsilon_b} \right)^2 \frac{1}{\sqrt{-\varepsilon_b \varepsilon_m}} h_f \Delta n \quad (S3)$$

One precondition of equation S3 is  $\Delta n = n_f - n_b \ll n_b$ . Considering that in general  $\Delta n = cdn/dc$ , it has

$$\Delta\theta \approx \frac{4\pi}{\lambda n_b^2 \cos\theta} \left( \frac{\epsilon_m \epsilon_b}{\epsilon_m + \epsilon_b} \right)^2 \frac{1}{\sqrt{-\epsilon_b \epsilon_m}} \frac{dn}{dc} \Delta m \quad (\text{S4})$$

where  $dn/dc$  is the refractive index increment,  $\Delta m = c_f h_f$  is the areal surface mass density.

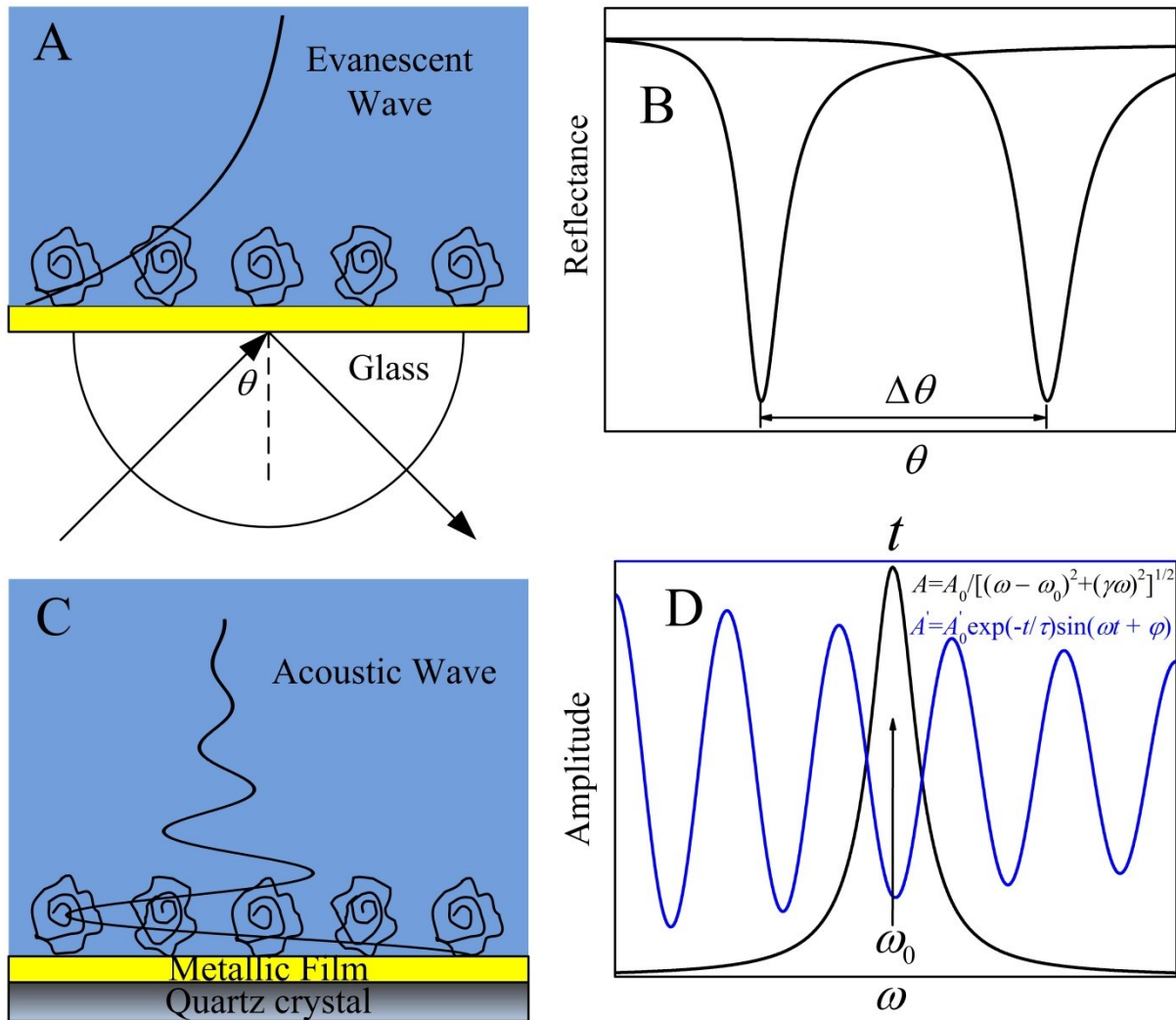


Figure S1. Schematic diagrams of QCM and SPR measurements. For SPR technique, the incident angle is increased to obtain the one at which the reflectance is the minimum (A and B). For QCM technique, the frequency dependent oscillation amplitude and the time dependence of resonant amplitude of quartz crystal are provided when the driving voltage is switched on and off, respectively (C and D).

Equation S2 is valid only for one single homogeneous layer. For polymers, surface concentration generally decreases with increasing distance to solid substrate.<sup>5,6</sup> In this case, the layer should be divided into  $u$  sub-layers. The 1st and  $uth$  layers contact with sensor surface and semi-infinite liquid, respectively. The expression of  $M$ -matrix is<sup>1</sup>

$$M = \left( \prod_{k=0}^u M_k \right)_{ij}$$

$$M_k = \begin{bmatrix} \cos(\beta_k) & -i \sin(\beta_k) / q_k \\ -i q_k \sin(\beta_k) & \cos(\beta_k) \end{bmatrix}$$

Quartz crystal microbalance comprises a thin quartz crystal sandwiched between two metal electrodes that establish an alternating electric field across the crystal, causing vibrational motion of the crystal at its resonant frequency. This resonant frequency is sensitive to mass change on top of the metal electrodes. In gas phase it generally has<sup>7</sup>

$$\Delta f = -\frac{f}{m_q} \Delta m \quad (S5)$$

where  $f$  and  $m_q$  are the resonant frequency and areal mass of quartz crystal, respectively. This is the well-known Sauerbrey equation. For commonly used 5 MHz quartz crystal, a 1 Hz in  $f$  indicates a 17.7 ng·cm<sup>-2</sup> in surface mass. In liquid phase, however, experimental results showed that with increasing  $\Delta m$ ,  $\Delta f/\Delta m$  either remains constant with the flexible values not smaller than  $-f/m_q$ ,<sup>8-10</sup> or decreases with different relation between  $\Delta f/\Delta m$  and  $\Delta m$  reported.<sup>11-</sup>

13

The rambling experimental results indicate the invalidity of Sauerbrey equation and call for the new theory. Among those developed in the past three decades,<sup>14-17</sup> the Voight model is the most widely used.<sup>15</sup> It introduces a new parameter, dissipation factor ( $D$ ), which is

measured as the decay in resonance amplitude that occurs when the driving voltage is switched off. The  $\Delta f$  and  $\Delta D$  induced by a homogeneous layer and a semi-infinite Newtonian liquid is

$$\Delta f \approx \text{Im}\left(\frac{\chi}{2\pi m_q}\right) \quad (\text{S6})$$

$$\Delta D \approx \text{Re}\left(\frac{\chi}{\pi f m_q}\right) \quad (\text{S7})$$

where

$$\chi = \kappa_f \xi_f \frac{1 - A \exp(2\xi_f h_f)}{1 + A \exp(2\xi_f h_f)}$$

$$A = \frac{\kappa_f \xi_f + \kappa_b \xi_b}{\kappa_f \xi_f - \kappa_b \xi_b}$$

$$\kappa = \mu - i \frac{\mu}{\omega} \quad \xi = \sqrt{-\frac{\rho \omega^2}{\mu + i \eta \omega}}$$

where  $\rho$ ,  $\eta$  and  $\mu$  are the density, viscosity and shear modulus, respectively,  $\omega = 2\pi f$  is the angular frequency.

For the longitudinal heterogeneous layer, it has

$$\chi = \kappa_1 \xi_1 \frac{1 - A_1 \exp(2\xi_1 h_1)}{1 + A_1 \exp(2\xi_1 h_1)}$$

with the value of  $k$  from 1 to  $u - 1$ , it has

$$A_k = \frac{\kappa_k \xi_k [1 + A_{k+1} \exp(2\xi_{k+1} h_{k+1})] - \kappa_{k+1} \xi_{k+1} [1 - A_{k+1} \exp(2\xi_{k+1} h_{k+1})]}{\kappa_k \xi_k [1 + A_{k+1} \exp(2\xi_{k+1} h_{k+1})] + \kappa_{k+1} \xi_{k+1} [1 - A_{k+1} \exp(2\xi_{k+1} h_{k+1})]}$$

and for  $k = u$

$$A_k = \frac{\kappa_k \xi_k - \kappa_b \xi_b}{\kappa_k \xi_k + \kappa_b \xi_b}$$

## SI 2: Dependences of SPR and QCM Signals on Properties of Modified Layer

Figures S2, S3 and S4 reveal the dependence of SPR and QCM signals on the properties (thickness, refractive index, viscosity, and their profiles) of layer above sensor surface. The data is calculated using Fresnel equation and Voight model, respectively.

Figure S2 shows that  $\Delta\theta$  and  $\Delta f$  increase proportionally with increasing layer thickness, and gradually approach a plateau, indicating that shear acoustic and evanescent waves are completely dissipated in the layer. One obvious difference is the proportional thickness regimes of  $\Delta\theta$  and  $\Delta f$  depend weakly and strongly on the properties of the film, respectively. This is easy to understand. From vapor, to liquid, to viscous mediums, and to solid films, the refractive index only increases by tens of percent, whereas viscosity increases by more than ten orders of magnitude. Therefore,  $l_d$  remains relatively constant at about 200 nm, but  $\delta$  expands from tens of nanometers to a macroscopic value (Table 1). The different values of  $l_d$  and  $\delta$  lead to the different propagation characters of evanescent and shear acoustic waves, as shown in Figure S5.

One difference between Figure S3A and S3B is that the sensitivity of  $\Delta\theta$  is independent of  $n$ , while the sensitivity of  $\Delta f$  to  $\eta$  decreases with increasing viscosity. These imply that  $\Delta\theta$  and  $\Delta f$  are inert and very sensitive to the refractive index and viscosity profiles of the film, respectively, as shown in Figure S5.

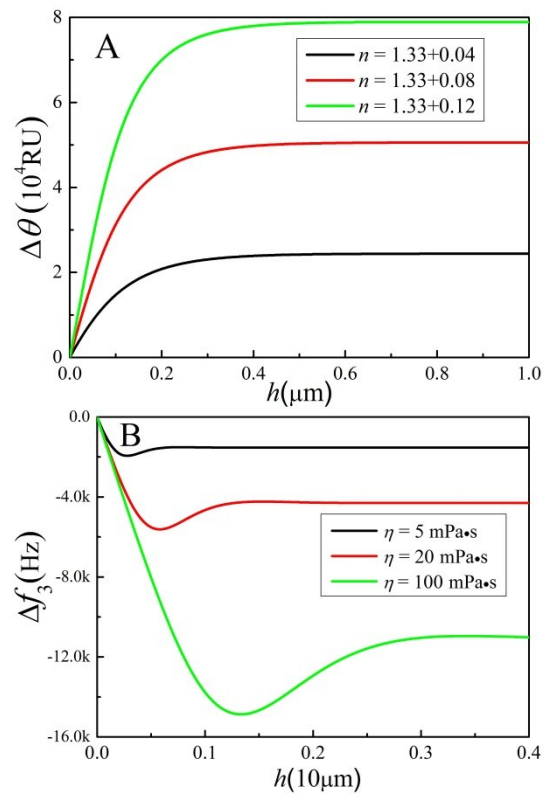


Figure S2. Calculated SPR and QCM responses versus the thickness for layer of different refractive indexes and viscosities, respectively. Properties of prism, metal film are the same as that in Figure 1, refractive index of bulk solution is 1.330.

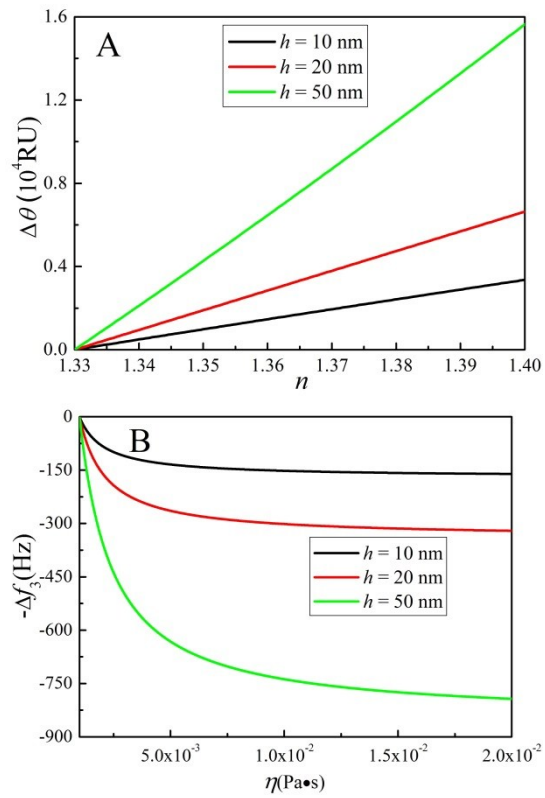


Figure S3. Calculated SPR (A) and QCM (B) responses versus the refractive index and viscosity, respectively, of a single layer of varying thicknesses. The parameters involved are the same as those in Figure S2.

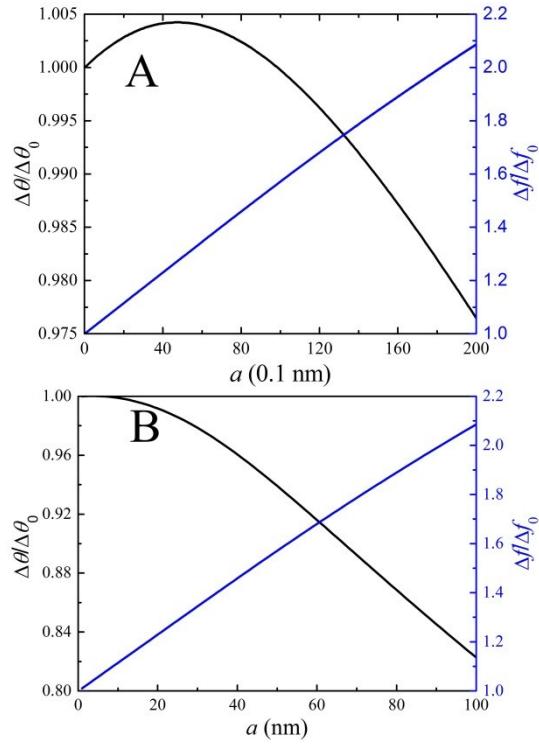
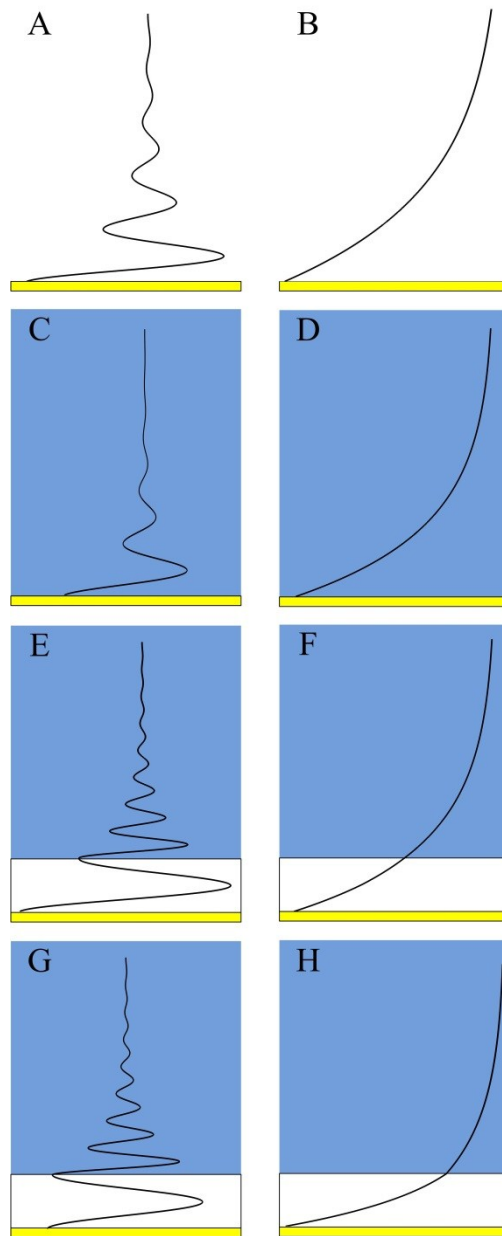


Figure S4. Responses of  $\Delta f$  and  $\Delta\theta$  to profiles of refractive index and viscosity, respectively. (a) Thickness of a homogeneous layer is supposed to be 20 nm. Profile follows  $x = x_b + (x_0 - x_b)\{1 - \tanh[(z - b)/a]\}/2$ , while  $z$  is the distance to the solid substrate,  $x$  can be concentration  $c$ ,  $\eta$  or  $n$ ,  $b = a \times \log[\exp(40 \text{ nm}/a) - 1]/2$  for maintaining a constant mass;  $\eta_b$ ,  $\eta_0$ ,  $n_b$ ,  $n_0$  are 0.001, 0.01 Pa·s and 1.330, 1.410, respectively. The thickness of every sub-layer is 0.1 nm. (b) The layer is 100 nm thick, and  $b = a \times \log[\exp(200 \text{ nm}/a) - 1]/2$ .

### SI 3

Figure S5 Propagation of shear acoustic and evanescent waves in different mediums, (A B) vapor phase, (C D) viscous boundary solutions, (E F) soft layer and viscous boundary solutions, (G H) solid layer and viscous boundary solutions.



References:

- (1) W. N. Hansen, *J. Opt. Soc. Am.*, 1968, **58**, 380
- (2) I. Pockrand, *Surf. Sci.*, 1978, **72**, 577
- (3) B. Liedberg, I. Lundstrom, E. Stenberg, *Sens. Actuators B*, 1993, **11**, 63-72.
- (4) L. S. Jung, C. T. Campbell, T. M. Chinowsky, M. N. Mar, S. S. Yee, *Langmuir*, 1998, **14**,

5636-5648.

- (5) S. T. Milner, *Science*, 1991, **251**, 905-914.
- (6) P. Auroy, Y. Mir, L. Auvray, *Phys. Rev. Lett.*, 1992, **69**, 93-95.
- (7) G. Sauerbrey, *Z. Phys.*, 1959, **155**, 206-222.
- (8) M. Muratsugu, F. Ohta, Y. Miya, T. Hosokawa, S. Kurosawa, N. Kamo, H. Ikeda, *Anal. Chem.*, 1993, **65**, 2933-2937.
- (9) T. Ozeki, M. Morita, H. Yoshimine, H. Furusawa, Y. Okahata, *Anal. Chem.*, 2007, **79**, 79-88.
- (10) H. Furusawa, T. Ozeki, M. Morita, Y. Okahata, *Anal. Chem.*, 2009, **81**, 2268-2273.
- (11) E. Reimhult, C. Larsson, B. Kasemo, F. Hook, *Anal. Chem.*, 2004, **76**, 7211-7220.
- (12) P. Bingen, G. L. Wang, N. F. Steinmetz, M. Rodahl, R. P. Richter, *Anal. Chem.*, 2008, **80**, 8880-8890.
- (13) I. Carton, A. R. Brisson, R. P. Richter, *Anal. Chem.*, 2010, **82**, 9275-9281.
- (14) Rodahl, M.; Kasemo, B. *Sens. Actuators A*, 1996, **54**, 448-456.
- (15) M. V. Voinova, M. Rodahl, M. Jonson, B. Kasemo, *Phys. Script.*, 1999, **59**, 391-399.
- (16) D. Johansmann, *Macromol. Chem. Phys.*, 1999, **200**, 501-516.
- (17) J. Kankare, *Langmuir*, 2002, **18**, 7092-7094.